Journal of Nepal Geological Society, 2013, Vol. 46, pp. 133-142

Double difference relocation of local earthquakes in the Nepal Himalaya

***S. Rajaure[1], S. N. Sapkota[1], L. B. Adhikari[1], B. Koirala[1], M. Bhattarai[1], D. R. Tiwari[1], U. Gautam[1], P. Shrestha[1], S. Maske[1] , J. P. Avouac[2], L. Bollinger[3] and M. R. Pandey[4]**

[1]Department of Mines and Geology, Nepal
[2]California Institute of Technology, USA
[3]Departement Analyse Surveillance Environnement, France
[4]Gyaneshwor, Kathmandu
*(*Email: srajaure@gmail.com)*

ABSTRACT

Interseismic strain across the Himalaya is associated with intense microseismic activity. In this study we analyze in detail this seismicity to explore in more details how it relates to Himalayan tectonics. We use the Double Difference Relocation Method to relocate local earthquakes recorded by National Seismological Centre in the period between 1995 and 2003. We also determined fault plane solutions for 10 earthquakes based on waveforms modeling and first P-motion data to complement the existing dataset of focal mechanisms. The results depict a narrow belt of intense seismic activity, at depth between 10 and 20km, which can be traced all along the topographic front of the Higher Himalaya in Nepal. This zone coincides with the zone of interseismic strain build up at the downdip end of the locked portion of the Main Himalayan Thrust fault. These earthquakes probably activate minor faults within the Himalayan wedge, in a volume which experiences stress build up in the interseismic period. The intense seismic activity generally cease abruptly as the elevation of topography gets higher than 3500 m. This elevation also coincides with a change of tectonic regime. Earthquakes within the seismicity belt at front of the Higher Himalaya are of thrust type indicating N-S shortening. Where the topographic elevation is higher than 3500 m focal mechanisms indicate E-W extension. The effect of topography on the regional stress field thus provides a simple explanation for the distribution of focal mechanisms and the seismicity cut-off at the 3500m elevation contour line.

Key words: Himalaya, Relative relocation, hypocenters, focal mechanisms.

Received: 8 November, 2012 **Revision accepted**: 14 June, 2013

INTRODUCTION

The Himalaya is one of the most active orogens in the world. It has resulted from the on-going collision of India and Eurasia which started about 50 million years ago (e.g., Avouac 2003). Today India keeps on moving north with respect to stable Eurasia at a rate of about 4 cm/yr (Bettinelli et al. 2006). Active deformation in the Himalaya is the cause for recurring devastating earthquakes. At least six earthquakes with magnitudes larger than 7.5 have occurred since 1897, including the Mw7.6 Kashmir earthquake with a death toll of about 85,000 (Ambraseys and Bilham 2000; Ambraseys and Douglas 2004; Avouac et al 2006). The largest among these earthquakes is the 1950 Assam earthquake which has released a moment magnitude estimated to be Mw8.5. Paleoseismic investigations indicate that even larger earthquakes may have happened in the past at various locations along the arc (Lave´ et al. 2005; Kumar et al. 2010).

The Himalaya of Nepal occupies approximately one-third of the total length of the arc and hosts the highest mountain peaks in the world. Seismic monitoring started there in the early 80s with the deployment of 5 stations around Kathmandu valley, which was extended by 1994 to a national network covering all of Nepal under a collaboration between the Departement of Mines and Geology of Nepal and the Departement Analyse Surveillance Environnement (DASE, France) (Pandey et al. 1995; Pandey et al. 1999) (Fig. 1). This network has revealed a belt of intense microseismic seismic activity following the front of the high Himalaya (Fig. 2).

In this study we discuss the characteristics and significance of this seismicity based on the data from

the national network of Nepal as well as from temporary deployment of seismic stations (Fig. 1). We use the double-difference technique (Waldhauser and Ellsworth 2000) to constrain better earthquake locations and waveform modeling (Zhao and Helmberger 1994) to determine earthquake focal mechanisms of a subset of events.

SEISMOTECTONIC SETTING

Active tectonics in the Himalaya is characterized by underthrusting of the Indian lithosphere beneath the chain along the Main Himalayan thrust (MHT) (Zhao et al. 1993) . This active structure emerges at the surface at the foot of the Himalaya (Fig. 3), where folding of Holocene terraces indicate a long term thrusting rate of 21+/-1.5mm/yr (Lavé and Avouac 2000). This rate is equal within uncertainties to the 19+/-2.5 mm/yr thrusting rate on the MHT determined from modeling geodetic deformation across the Himalaya (Bettinelli et al. 2006).

The pattern of geodetic strain across the Himalaya indicates that the MHT is actually locked from the surface to beneath the high Himalaya over a width of about 100 km (Bilham et al. 1997; Ader et al. 2012). Slip along the locked portion of the MHT must occur during transient slip event, presumably the large Himalayan earthquakes. It has been shown that the belt of microseismic activity actually occurs at the downdip end of the locked fault zone where stress builds up in the interseismic period (Cattin and Avouac 2000; Bollinger et al. 2004).

Due to the linear distribution of seismic stations, earthquake locations and depths are poorly constrained from standard travel-time location techniques so that the details of how this seismicity relates to the Himalayan structures remain uncertain. For example, it is unclear from standard locations whether the seismicity is clustered around the MHT or distributed in a volume of significant dimension. Furthermore, a better resolved 3D geometry of the mid crustal microseismic cluster could help reveal secondary features within the Himalayan wedge.

RELOCATION OF LOCAL SEISMICITY

The accuracy of routinely estimated absolute hypocenter locations is influenced by many factors, such as the network geometry, available arrival time data, arrival-time reading accuracy, and knowledge of the crustal structure (Pavlis 1986; Gomberg et al. 1990). As a result, the uncertainty in the location of routinely determined hypocenters is typically many times larger than the source dimension of the events (Waldhauser 2001). The double Difference technique is an efficient method to determine high-resolution hypocenter locations over large distances (Got et al. 1994; Waldhauser and Ellsworth 2000). This technique has been used widely and proved quite helpful to help delineate active seismic structures (e. g., Wu et. al. 2004; Yukutake et. al. 2007; Waldhauser and Ellsworth 2000; Waldhauser et. al. 2004).

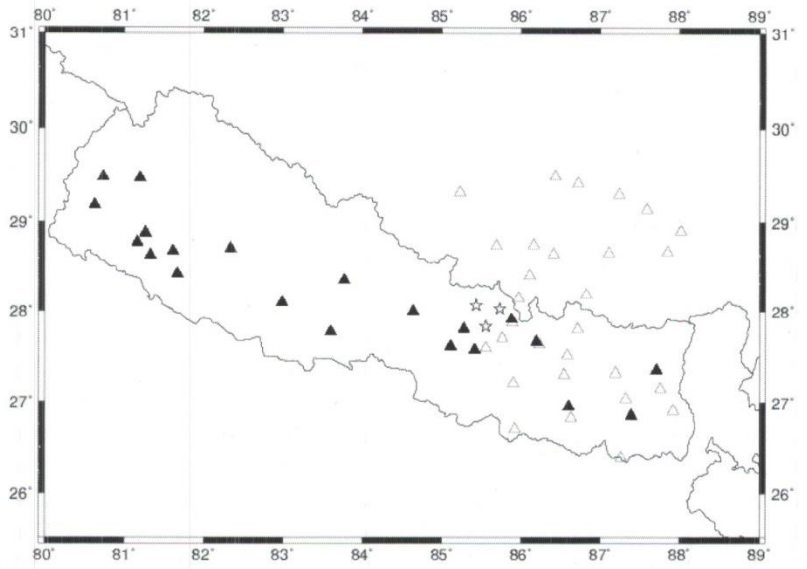

Fig. 1: Distribution of seismic stations used in this study. The permanent short period 1-component (vertical) stations are shown as solid triangles. The open stars show location of 3-component short period stations deployed in 1995 and the open triangles show locations of broadband 3-component stations deployed as part of the HIMNT experiment between 2001 and 2003 (e.g., Monsalve et al. 2006; Sheehan et. al. 2008).

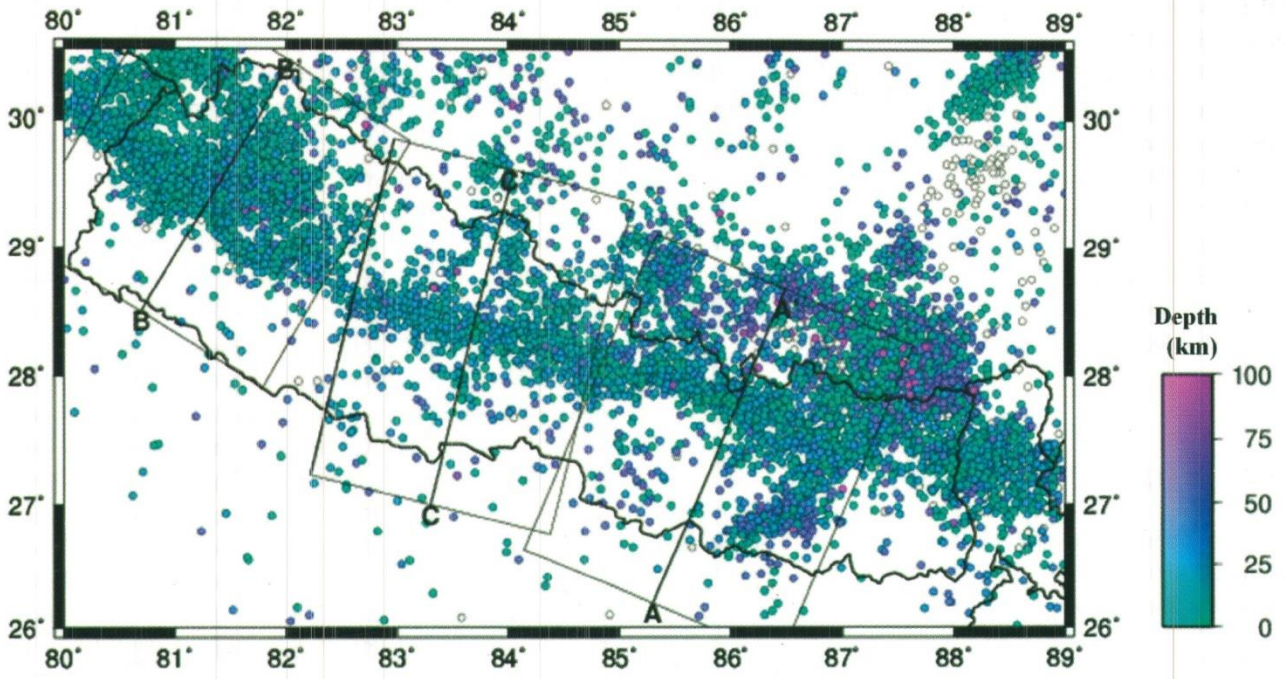

Fig. 2: Seismicity in and around Nepal recorded by the National Seismological Center of Nepal. Earthquakes recorded between 1995 and 2003 with local magnitude larger than 1.0 are shown. AA' and BB' show location of sections in Fig. 3.

Seismicity associated with creeping fault (where most of the slip is actually aseismic) has in particular revealed to form linear streaks within a very narrow fault zone as has been observed for the Parkfield segment of the San Andreas Fault (Waldhauser et. al. 2004) and for the Hayward Fault (Waldhauser and Ellsworth 2000).

Method

The double difference relocation technique is a relative relocation algorithm, where groups of earthquakes are relocated relative to each other. If the hypocentral separation between two earthquakes is small in comparison to the event-station distance and the scale length of velocity heterogeneities, then the ray paths between the source region and a common station are similar along almost the entire ray path. In this case, the difference in the travel times for two events observed at one station can be attributed to the spatial offset between the events with high accuracy (Got et al. 1994; Waldhauser and Ellsworth 2000).

Double Difference equations are constructed by differencing Geiger's equation for earthquake location. In this way, the residual between observed and calculated travel-time difference (or double-difference) between two

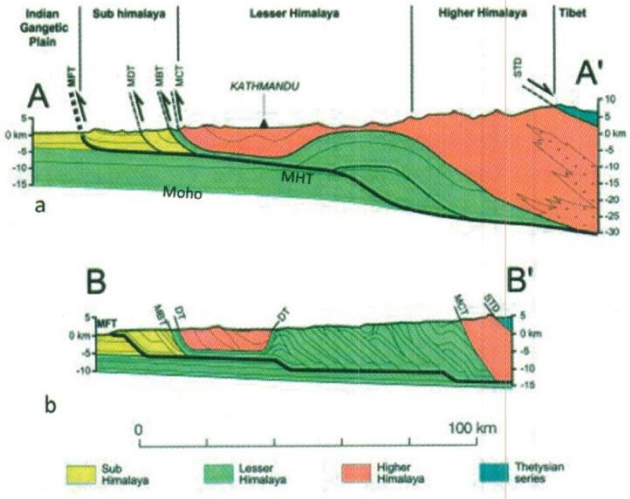

Fig. 3: (a) Simplified geological section across the Himalaya of central Nepal (AA' in Figure 2). (b) Geological section across the Himalaya of Far-Western Nepal (BB' in Figure 3) (modified from Pandey et al. 1999).

events at a common station are related to the adjustments in the relative position of the hypocenters and origin times through the partial derivatives of the travel times for each event with respect to the unknown (latitude, longitude, depth, and origin time). HypoDD, the program used in this study, implements the double difference earthquake location algorithm of Wadahauser and Ellsworth (2000). It calculates travel times in a layered velocity model (where velocity depends only on depth) for the current hypocenters at the station where the phase was recorded. In this method the residuals in arrival times between events i and j (double difference) recorded at the k^{th} station are used. They are defined as:

$$dr_k^{ij} = \left(t_k^i - t_k^j\right)^{obs} - \left(t_k^i - t_k^j\right)^{cal} \quad (1)$$

where 'obs' stands for observed, and 'cal' stands for calculated arrival times. For two events i and j at the k^{th} station, we may write:

$$\frac{\partial t_k^i}{\partial m}\Delta m^i - \frac{\partial t_k^j}{\partial m}\Delta m^j = dr_k^{ij} \quad (2)$$

Where Δm_i is the corrections vector of the hypocentral parameters (dx, dy, dz and dt) for event i; if the events are very close, then the same slowness can be used and the equation becomes:

$$\frac{\partial t_k^i}{\partial m}\Delta m^{ij} = dr_k^{ij} \quad (3)$$

In DD relocation, the common mode errors, related to the receiver-side structure, cancel. Thus the need of station corrections or predicted travel times for the portion of raypath that lies outside the focal volume is avoided. The dense distribution of earthquakes within Nepal mid-crustal cluster make therefore the use of this technique particularly promising.

Application to the seismicity of Nepal

The National Seismological Centre of the Department of Mines and Geology (DMG) operates a nationwide seismic network (Fig. 1) consisting primarily of 21 vertical component short period sensors (ZM500) in collaboration with the Departement Analyse Surveillance Environnement (DASE), France. We used the seismicity catalogue produced by the DMG for the period 1995-2003, a period of optimal functioning of the network.

We have used arrival time data of P- and S- waves from earthquakes initially located between 26°N and 30.5°N latitude and 80°E and 88.5°E longitude (Fig. 2). The data consists of arrival time data of earthquakes, their initial locations and hypocenters determined from a local 1-D velocity model (Rajaure 2002). The velocity model was derived using Crosson (1976) technique for simultaneous inversion of travel time data for velocity structure and hypocenters of local earthquakes which occurred in western Nepal. This velocity model is in close agreement with the velocity model of Pandey (1985), which was derived using minimum apparent velocity technique using data from central Nepal. We selected earthquakes with magnitude greater than or equal to 1.0 localized by at least by 3 stations and with at least 5 arrival times (S and P waves). First, the local earthquakes were relocated using the HYPOCENTER tool of SEISAN software after implementing Rajaure (2002) velocity model (Figs. 5b, 6b and 7b). This step helped, respectively, to remove poor quality data and corrected seismic events depth distribution accordingly to the new velocity model. Then the arrival time data and the hypocenters were used as input data in the double difference relocation (Waldhauser 2001) to relocate the earthquakes in group. During data selection the inter event spacing was selected 10 km and the event-source distance was chosen to 400 km. We have used about 12000 earthquakes in this study and about 7000 events, more than half, were relocated successfully. The relocated seismicity is shown in map view in Fig. 4 and cross sections in Figs. 5c, 6c and 7c.

Comparison between the original catalogue and the relocated catalogue shows that epicenters have been moved typically by 7.5 km (which is the variance of the distributions of distance between original and relocated epicenters) and depth by typically 15 km (which is the variance of the distributions of depths between original and relocated hypocenters). Before the relocation the uncertainty associated with the routinely determined hypocenters were larger than 5 km on average and after the double difference relocation it dropped down up to a few hundred meters.

Fig. 8 shows the distribution of seismicity along a section running through Kathmandu valley. Here it is possible to compare our relocated seismicity with a subset of well located events. In 1997, the network was augmented with 3 three-component short period seismometers in the north of the Kathmandu Valley (open stars in Fig. 1) for a period of about six months. These stations were deployed specifically in order to better constrain the depths of earthquake-foci occurring in the north of Kathmandu. The comparison between the two catalogues shows an excellent agreement (Fig. 8).

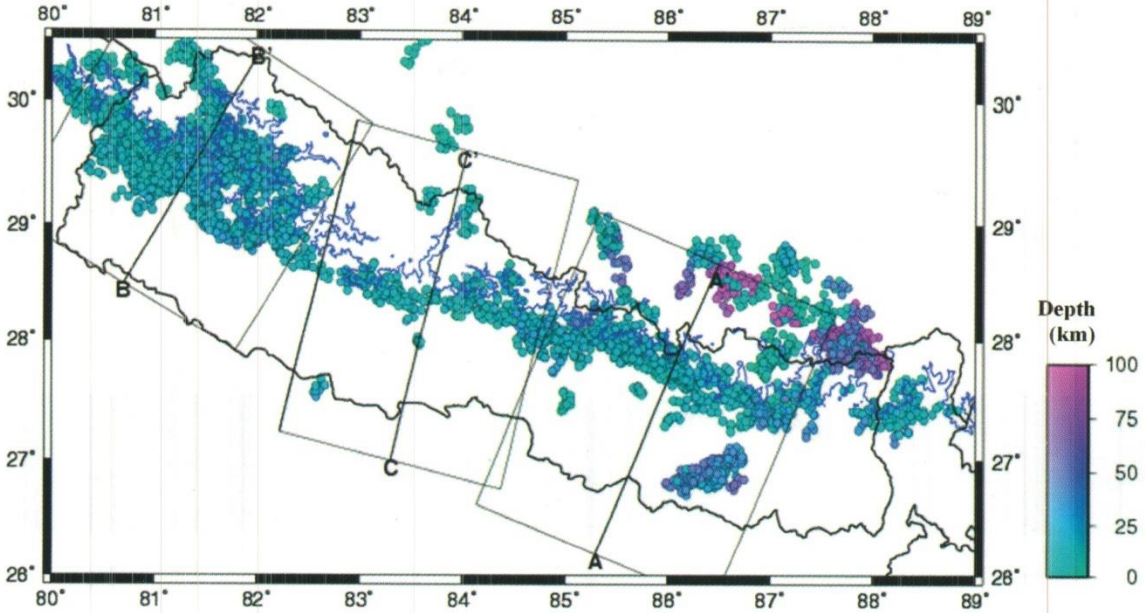

Fig. 4: Relocated seismicity. Note that the relocated epicenters are more clustered than in the original catalogue. The blue line shows the 3500 m elevation contour line for reference. In particular the clustering of seismicity along the front of the high range is reinforced. It confirms that this belt of seismicity abruptly ends at the 3500 m elevation contour line (Avouac 2003; Bollinger et al. 2004). The earthquakes in this seismicity belt have shallow foci, where the depth ranges between 10 and 25 km (Figs. 5c, 6c and 7c). Lower crust to upper mantle earthquakes are observed in the 1988 Udayapur Earthquake (M6.5) area and South Tibet (Fig. 5c). Seismicity pattern is simple in the east of 82 E where the belt is characterized by a narrow belt whereas in the west of 82 E, seismicity is distributed into two sub parallel belts.

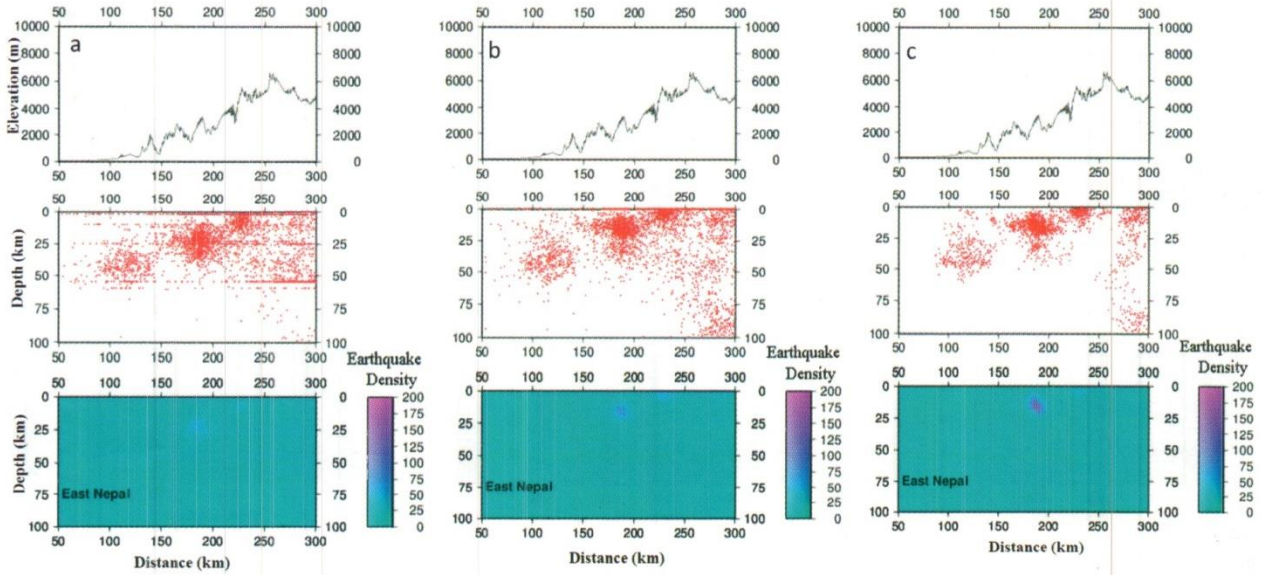

Fig. 5: Distribution of seismicity along section AA' (Fig. 4) across the Himalaya of eastern Nepal. The rectangle centered on section AA' in Fig. 4 shows the swath within which all earthquakes are projected on a vertical plane along AA'. The earthquake foci are from NSC's location (a), SEISAN relocation (b) and double difference relocation (c). The upper panel is the topography along the profile. The middle panel is the foci distribution and the lower panel shows the density of earthquake foci in a 2x2 km grid.

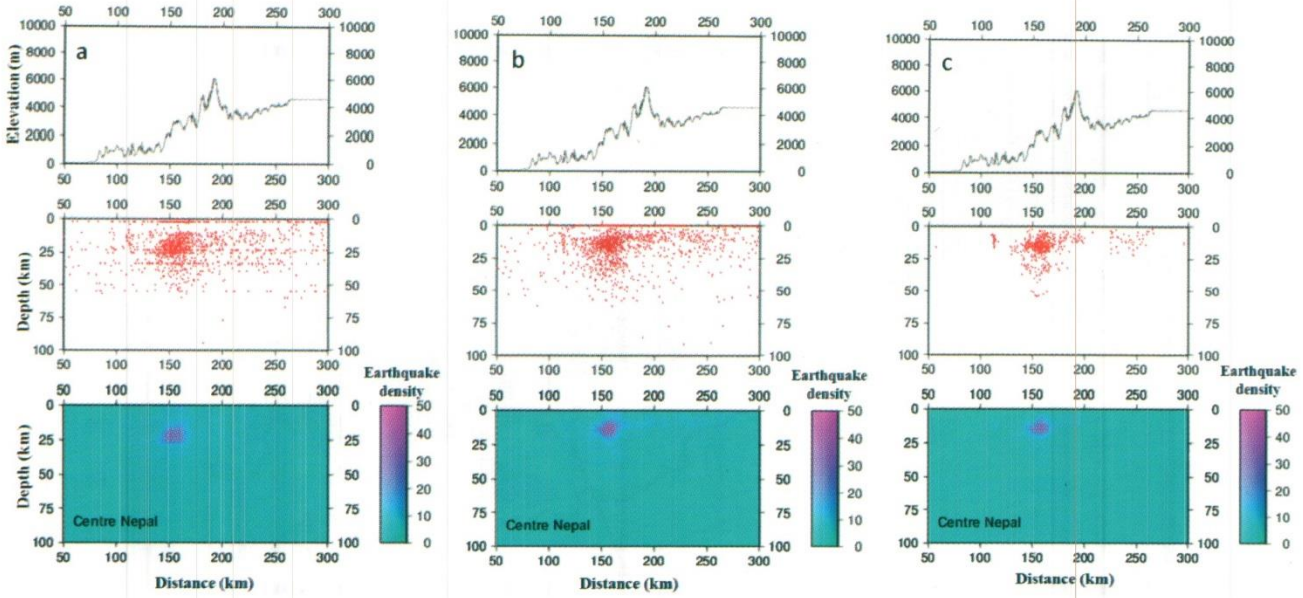

Fig. 6: Distribution of seismicity along section CC' (Fig. 4) across the Himalaya of central Nepal. The rectangle centered on section CC' in Fig. 4 shows the swath within which all earthquakes are projected on a vertical plane along CC'. The earthquake foci are from NSC's location (a), SEISAN relocation (b) and double difference relocation (c). The upper panel is the topography along the profile. The middle panel is the foci distribution and the lower panel shows the density of earthquake foci in a 2x2 km grid.

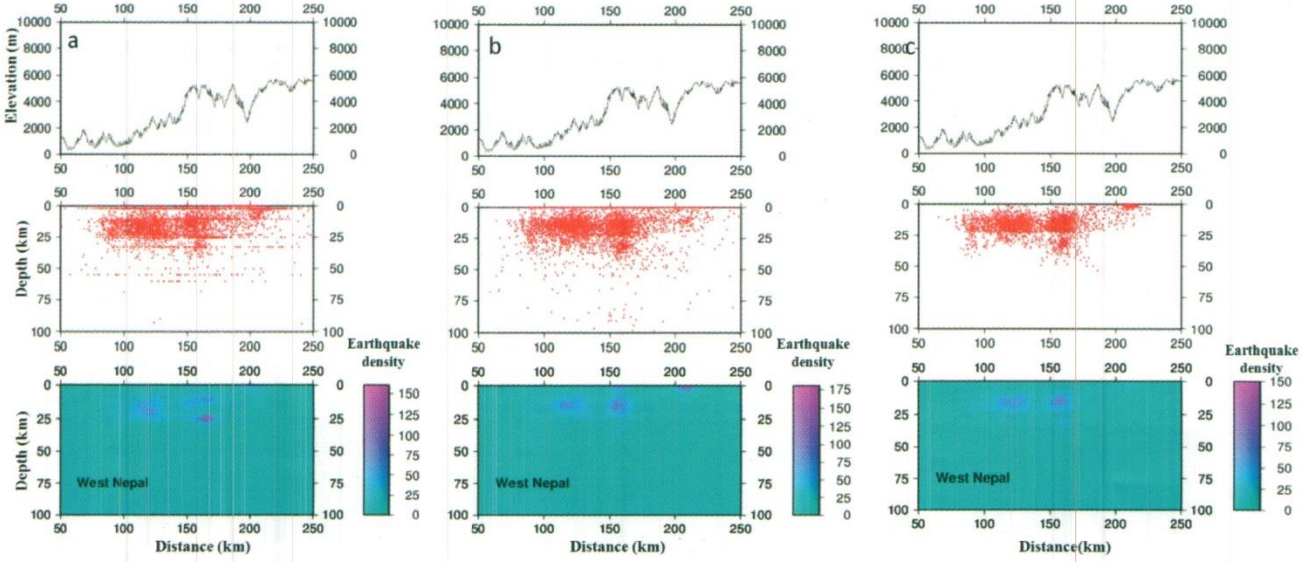

Fig. 7: Distribution of seismicity along section BB' across the Himalaya of far-western Nepal. The rectangle centered on section BB' in Fig. 4 shows the swath within which all earthquakes are projected on a vertical plane along BB'. The earthquake foci are from NSC's location (a), SEISAN relocation (b) and double difference relocation (c). The upper panel is the topography along the profile. The middle panel is the foci distribution and the lower panel shows the density of earthquake foci in a 2x2 km grid.

FOCAL MECHANISMS DETERMINATION

To complement the existing dataset of focal mechanisms (black focal spheres in Fig. 11), we determined additional focal mechanisms for 10 events (Fig. 11). We used polarities of P-waves (from National Seismological Network of Nepal) at all the stations available (Fig. 1) and were able to obtain well constrained solution for 6 of them. Four additional solutions, for which the polarity data were insufficient, were determined using the waveform modeling technique of Zhao and Helmberger (1994) on broadband data from HIMNT network. This technique called 'Cut and Paste (CAP)' breaks waveform into P and surface waves and inverts them independently. This method desensitizes the effect of velocity model inaccuracy and lateral crustal variation.

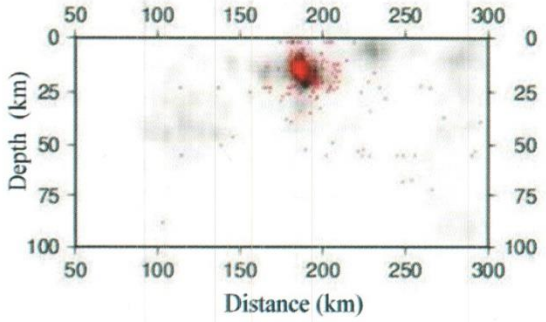

Fig. 8: Distribution of seismicity along section AA' in Fig. 4. Density of earthquakes according to our relocated catalogue is compared with the hypocenters (red dots) determined from standard travel time location procedure but using 3 additional 3-component seismic stations deployed in 1997.

DISCUSSION

This analysis confirms and refines number of features which had been pointed to in previous studies (e. g. Pandey et. al. 1995; Pandey et. al. 1999; Monsalve et. al. 2006; Sheehan et. al. 2008).

First a significant fraction of Nepal seismicity is well clustered at depths between 10 and 20 km along a belt following the front of the high Himalaya (Figs. 4). The focal mechanisms indicate N-S compression there (Fig. 11 and 12) consistent with N-S shortening across the Himalaya as measured from Geodesy or indicated by the active thrust faults at front of the sub-Himalaya.

This seismicity belt coincides remarkably well with the zone of interseismic stress buildup at the downdip end of the locked portion of the Main Himalayan Thrust fault (Bollinger et. al. 2004). The seismicity belt abruptly ends to the North at the 3500 m elevation contour line, except at a few places where cluster of normal events are observed. The topographic control on seismicity suggests, as pointed out to by (Avouac 2003; Bollinger et. al. 2004), that at elevation lower than 3500 m the maximum compressive stress is oriented North South, so that the Coulomb stress increases in the interseismic period as N-S compressions increases (Bollinger et al. 2004), while at elevation higher than 3500 m the maximum stress is vertical favoring normal faulting. In that situation thrust events are inhibited while normal events are triggered at places where the divergence of thrusting along the Himalayan arc induces E-W extension as the modeling of Bollinger et al. (2004) shows. This

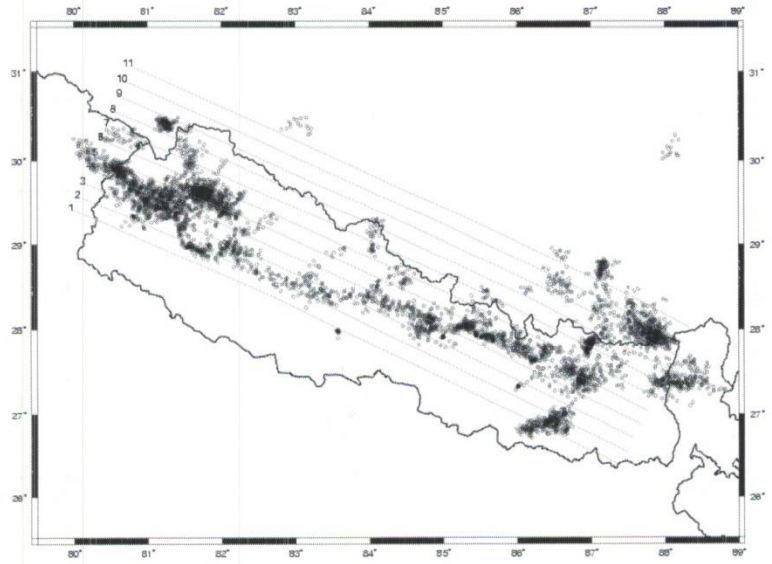

Fig. 9: Profile lines in NW-SE direction parallel to the seismicity belt. Sections in Fig. 10 are plotted along these lines from NW to SE direction.

topographic control of the tectonic regime is evidenced in Fig. 12 where focal mechanisms are plotted as a function of the elevation at their epicenter. The transition from thrust events to normal events is indeed observed to occur at an elevation of 3500 m.

Closer inspection of the seismicity belt shows that it occurs within a significant volume rather than being clustered along a well defined fault zone. So it seems that only a fraction of these events occur along the MHT. They most probably reflect activation of minor faults in the volume at the tip of the creeping portion of the MHT where the Coulomb stress is increased in the interseismic period.

Interesting details can additionally be noticed on the relocated seismicity map (Fig. 4) as well as on the cross sections (Figs. 5, 6, 7, 9 and 10). The seismicity belt is narrow east of 82°E, whereas in the west it is divided into two sub-parallel belts which merge again west of 80°E (Figs. 5, 6 and 7). Furthermore, cross sections parallel to the high range (sections 2, 3, 4 and 5 from Fig. 10) through Far Western Nepal suggest that this complex seismic cluster may dip toward the East in that region characterized by a complicated imbrication of thrust sheets (Fig. 3b).

Our seismicity catalogue also sheds light on deep seismicity beneath the northern edge of Gangetic plain south of Everest, an area which shows lower crust and upper mantle seismic activity (Fig. 4). This area coincides with the location of the 1988 (M6.5) Udayapur Earthquake, a major complex seismic event that occurred at more than 45 km within the lower indian crust (e.g., Chen and Kao 1996; Ghimire and Kasahara 2007). Our relocated catalogue shows that seismicity spreads across the Moho, as also observed by previous authors (Pandey et al. 1999; Monsalve et al. 2006), indicating that the rheology of the lower crust and upper mantle is actually brittle in that area.

CONCLUSIONS

The result shows a narrow belt of microseismic activity at the front of the Higher Himalaya at midcrustal depth. While clustered this seismicity does not seem to occur only on the MHT. It occurs within a finite volume where minor faults are probably reactivated due to interseismic stress build up. The main seismicity belt ends at the 3500 m elevation contour line demonstrating a strong topographic control of the tectonic regime, also seen independently in the focal mechanisms distribution. Deep earthquakes in southern part of Eastern Nepal and in Southern Tibet span the Moho

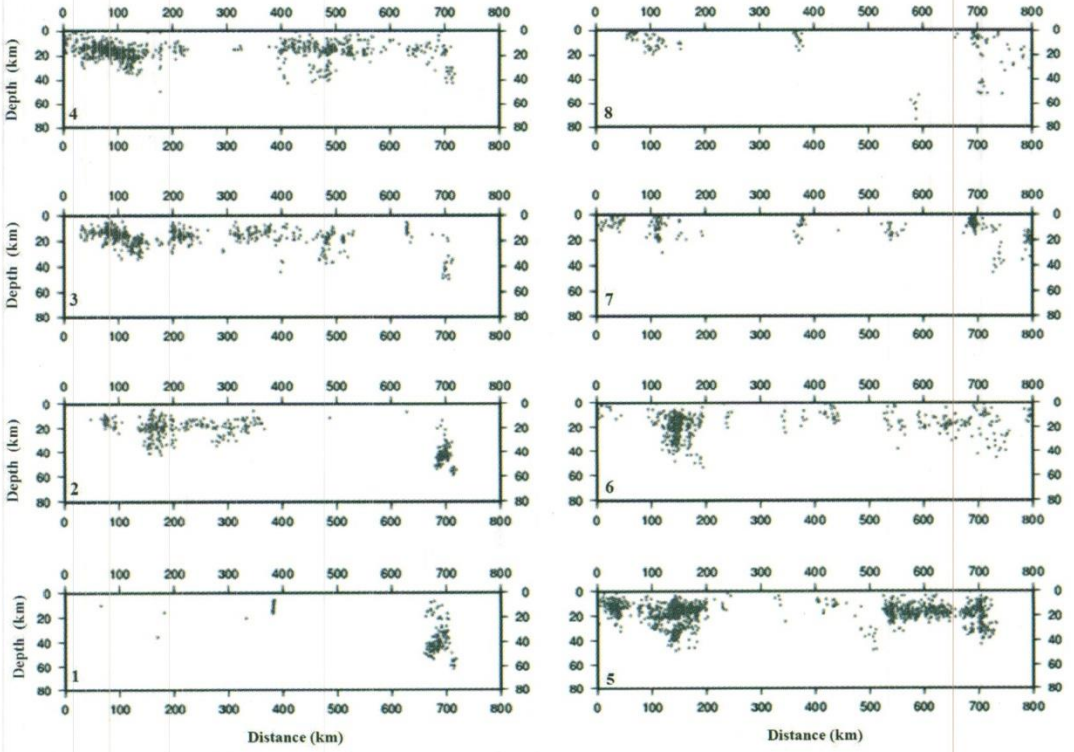

Fig. 10: Sections parallel to the seismicity belt (Fig. 9). Note that in 2, 3, 4 and 5, the far western Nepal seismic cluster seems to dip toward the East. Relatively deep earthquakes, approximately 700 km East from the beginning of the cross section correspond to aftershock area of 1988 Udayapur Earthquake.

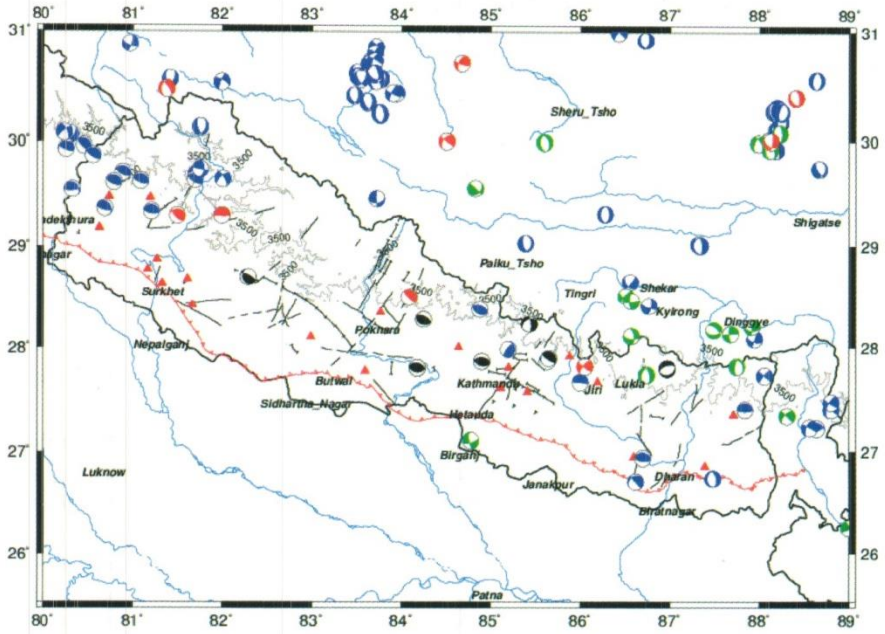

Fig. 11: Focal mechanisms of earthquakes in the Nepal Himalaya and southern Tibet with active faults (modified from Armijo et. al. 1986; Nakata 1989). Black focal spheres: first motion determinations (this study), red focal spheres: determinations from waveforms modeling (this study), light green focal spheres: waveform modeling (de la Torre et al. 2007), blue focal spheres: CMT Harvard catalogue, grey line is the 3500 m elevation contour line, the red line is Main Frontal Thrust (MFT).

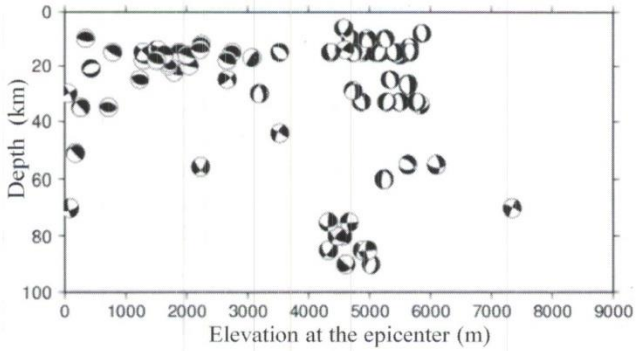

Fig. 12: Distribution of focal mechanisms (represented in map view) in depth according to the topographic elevation at the epicenter (x-axis) and hypocentral depth (y-axis).

demonstrating the brittle behavior of both the lower crust and upper Mantle.

ACKNOWLEDGEMENTS

We would like to thank the seismic network of Department of Mines and Geology which collected and made the data available for this study. Special thanks go to Mr. N. R. Sthapit, former Director General of Department of Mines and Geology, Nepal and Mr. R. K. Aryal, former Chief of National Seismological Centre, Nepal for their continuous support during this study.

REFERENCES

Ader, T., Avouac, J. P., Liu-Zeng, J., Lyon-Caen, H., Bollinger, L., Galetzka, J., Genrich, J., Thomas, M., Chanard, K., Sapkota, S. N., Rajaure, S., Shrestha, P., Ding, L. and Flouzat, M., 2012, Convergence rate across the Nepal Himalaya and interseismic coupling on the Main Himalayan Thrust: Implications for seismic hazard. Journal of Geophysical Research-Solid Earth, v. 117.

Ambraseys, N. and Bilham, R., 2000, A note on the Kangra earthquake of 4 April 1905. Current Science, v. 79, pp. 46–50.

Ambraseys, N. and Douglas, A., 2004, Magnitude calibration of North Indian earthquakes. Geophysical Journal International, v. 159, pp. 165-206.

Armijo, R., Tapponnier, P., Mercier, J. L., and Tonglin, H., 1986, Quaternary extension in

Avouac, J. P. A., 2003, Mountain building, erosion and the seismic cycle in the Nepal Himalaya. Advances in Geophysics, v. 46, 80 p.

Avouac, J. P., F. Ayoub, S. Leprince, O. Konca, and D. V. Helmberger, 2006, The 2005, Mw 7.6 Kashimir earthquake: Sub-pixel correlation of ASTER images and seismic waveforms analysis, Earth and Planetary Science Letters, vol. 249, pp. 514-528.

Bettinelli, P., Avouac, J. P., Flouzat, M., Jouanne, F., Bollinger, L., Willis, P. and Chitrakar, G. R., 2006, Plate motion of India

and interseismic strain in the Nepal Himalaya from GPS and DORIS measurements. Journal of Geodesy, v. 80, pp. 567–589.

Bilham, R., Larson, K., Freymueller, J. and members, P. I., 1997, GPS measurements of present-day convergence across the Nepal Himalaya. Nature, v. 386, pp. 61–64.

Bollinger, L., Avouac, J. P., Cattin, R. and Pandey, M. R., 2004, Stress build up in the Himalaya. Journal of Geophysical Research, 109, B11405, doi:10.1029/2003JB002911.

Cattin, R. and Avouac, J.-P., 2000, Modeling of mountain building and the seismic cycle in the Himalaya of Nepal. Journal of Geophysical Research, v. 105, pp. 13389–13407.

Chen, W. P. and Kao, H., 1996, Seismotectonics of Asia: some recent progress. In: Yin, A., Harrison, M. (Eds.) The tectonic of Asia. Cambridge University Press, pp. 37-62.

Crosson, R. S., 1976, Crustal structure modeling of earthquake data; 1, Simultaneous least squares estimation of hypocenter and velocity parameters. Journal of Geophysical Research, v. 81, pp. 3036-3046.

de la Torre, T. L, Monsalve, G., Sheehan, A., Sapkota, S., Wu, F., 2007, Earthquake processes of the Himalayan collision zone in eastern Nepal and the southern Tibetan Plateau. Geophysical Journal International, vol.171, pp. 718-738.

Ghimire S. and M. Kasahara, 2007, Source process of the Ms=6.6, Udayapur earthquake of Nepal-India border and its tectonic implication. Jour. Asian Earth Sci., v. 31 (2), pp. 128-138

Gomberg, J. S., Shedlock, K. M. and Roecker, S. W., 1990, The effect of S-wave arrival times on the accuracy of hypocenter estimation. Bulletin of Seismological Society of America, v. 80, pp. 1605–1628.

Got, J.-L., Fre´chet, J. and Klein, F. W., 1994, Deep fault plane geometry inferred from multiplet relative relocation beneath the south flank of Kilauea. Journal of Geophysical Research, v. 99, pp. 15,375–15,386.

Harvard University Department of Geological Sciences, 2005. Centroid Moment Tensor Catalog, www.seismology.harvard.edu/CMTsearch.html

Kumar, S., Wesnousky, S.G., Jayangondaperumal, R., Nakata, T., Kumahara, Y. & Singh, V., 2010. Paleoseismological evidence of surface faulting along the northeastern Himalayan front, India: Timing, size, and spatial extent of great earthquakes. Journal of Geophysical Research-Solid Earth, v. 115, B12422, doi:10.1029/2009JB006789.

Lave, J., Avouac, J. P., 2000, Active folding of abandoned Fluvial Terraces across the Siwalik Hills (Nepal). Journal of Geophysical Research, v. 105, pp. 5735-5770

Lave´, J., Yule, D., Sapkota, S., Basant, K., Madden, C., Attal, M. and Pandey, R., 2005, Evidence for a Great Medieval Earthquake (1100 A.D.) in the Central Himalayas, Nepal. Science, vol. 307, pp. 1302–1305.

Monsalve, G., Sheehan, A., Schulte-Pelkum, V., Rajaure, S., Pandey, M. R. and Wu, F., 2006, Seismicity and one dimensional velocity structure of the Himalayan collision zone: Earthquakes in the crust and upper mantle. Journal of Geophysics Research, v. 111, 19 p.

Nakata, T., 1989, Active faults of the Himalaya of India and Nepal. Special paper, Geological Society of America, v. 232, pp. 243-264.

Pandey, M. R., 1985, Seismic Model of Central and Eastern Lesser Himalayas of Nepal. Journal of Nepal Geological Society, v. 3(1 and 2), pp. 1-11.

Pandey, M. R., Tandukar, R. L. P., Lave, J. P. and Massot, J. P., 1995, Interseismic Strain Accumulation on the Himalayan Crustal Ramp, Nepal. Geophysical Research Letters, v. 22 (7), pp. 751-754.

Pandey, M. R., Tandukar, R. P., Avouac, J. P., Vergne, J., Heritier, T., 1999, Seismotectonics of the Nepal Himalaya from a local seismic network. Journal of Asian Earth Sciences, v. 17, pp. 703-712.

Pavlis, G. L. 1986, Appraising earthquake hypocenter location errors: a complete, practical approach for single-event locations, Bulletin of Seismological Society of America, v. 76, pp. 1699–1717.

Rajaure, S. 2002, One dimensional seismic velocity structure beneath western Nepal. Journal of Nepal Geological Society, v. 27 (special issue), pp. 119-122.

Sheehan, A. F., de la Torre, T., Monsalve, G., Schulte-Pelkum, V., Bilham, R., Blume, F., Bendick, R., Wu, F., Pandey, M. R., Sapkota, S., Rajaure, S., 2008, Earthquakes and crustal structure of the Himalaya from the Himalayan Nepal Tibet seismic experiment (HIMNT). Journal of the Nepal Geological Society, v. 38, p 8.

Southern Tibet. Journal of Geophysical Research, v. 91, pp. 13803–13872.

Waldhauser, F. and Ellsworth, W. L., 2000, A Double-Difference Earthquake Location Algorithm: Method and Application to the Northern Hayward Fault, California. Bulletin of Seismological Society of America, v. 90, no. 6, pp. 1353-1368.

Waldhauser, F., 2001, hypoDD -- A Program to Compute Double-Difference Hypocenter Locations. U. S. Geol. Survey, Open file Report. 01-113, pp. 25.

Waldhauser, F., Ellsworth, W. L., Schaff, D. P. and Cole, A., 2004, Streaks, multiplets, and holes: High-resolution spatio-temporal behavior of Parkfield seismicity. Geophysical Research Letters, v. 31, 4 p.

Wu, F. T., Chang and Wu, Y. M., 2004, Precisely Relocated Hypocenters, Focal Mecahnisms and Active Orogeny in Central Taiwan, Aspects of the Tectonic Evolution of China. Geological Society of London, Special Publication, v. 226, pp. 333-353.

Yukutake, Y., Takeda, T. and Obara, K., 2007, Well-resolved hypocenter distribution using the double-difference relocation method in the region of the 2007 Chuetsu-oki Earthquake. Letter-Earth-Planets Space, v. 60, pp. 1105-1109.

Zhao, L. S. and Helmberger, D. V., 1994, Source estimation from broadband regional seismograms. Bulletin of Seismological Society of America, v. 84, pp. 91-104.

Zhao, W., Nelson, K. D. and project INDEPTH Team, 1993, Deep seismic-reflection evidence of continental underthrusting beneath southern Tibet. Nature, v. 366, pp. 557–559.